Extinguishing pool fires with aqueous ferrocene dispersions containing gemini surfactants

Yusuke Koshiba [a,] *, Hideo Ohtani [b]

[a] Department of Materials Science and Chemical Engineering, Faculty of Engineering, Yokohama National University, 79-5 Tokiwadai, Hodogaya-ku, Yokohama 240-8501, Japan

[b] Department of Safety Management, Faculty of Environmental and Information Sciences, Yokohama National University, 79-7 Tokiwadai, Hodogaya-ku, Yokohama 240-8501, Japan

* Corresponding author: Telephone number: +81 45 339 3985

Fax number: +81 45 339 3985

E-mail address: ykoshiba@ynu.ac.jp

Complete postal address: 79-5 Tokiwadai, Hodogaya-ku, Yokohama 240-8501, Japan

Abstract

The objective of the present study was to explore the relationship between the dispersibility and fire-extinguishing capability of aqueous ferrocene dispersions containing gemini surfactants belonging to the same series, namely, olfin E1020, olfin PD 201, and surfynol 465. In this study, the dispersibility and ability to suppress pool fires were characterized by turbidity and extinguishing time, respectively. Ultrasonication enabled easy preparation of the aqueous dispersions of ferrocene powder containing the gemini surfactants. Visual observations and turbidity measurements clearly demonstrated that the order of dispersibility was as follows: ferrocene dispersion containing surfynol 465 ≥ ferrocene dispersion containing olfin E1020 > ferrocene dispersion containing olfin PD201. Fire suppression experiments indicated that the ferrocene diameter, in the ferrocene diameter range of 10.4–21.5 μm, negligibly influenced the extinguishing time. Furthermore, for the same ferrocene samples as were used for the turbidity measurements, the order of extinguishing ability was as follows: ferrocene dispersion containing surfynol 465 > ferrocene dispersion containing olfin E1020 > ferrocene dispersion containing olfin PD201; thus, the extinguishing ability was identical to the dispersibility order.

Keywords: Ferrocene; Fire extinguishing agent; Aqueous dispersion; Water mist; Gemini surfactant; Additive

1. Introduction

Over the past two decades in Japan, the number of fires in industrial facilities storing and handling dangerous goods (e.g., flammable liquids) has gradually increased, despite a decrease in the number of such facilities over the same period (FDMA, 2014). Accidental fires can cause deaths and injuries as well as severe economic loss; for instance, in 2013, 188 fires in industrial facilities were reported in Japan, causing 10 deaths, 60 injuries, and property loss of approximately 4.4 hundred million yen. Therefore, an effective fire-extinguishing agent for Class B fires is needed. A number of studies have been reported on such agents, including dry chemicals (Kuang et al., 2008), foam (Wang, 2014), pure water mist (Jenft et al., 2014), and water mist with additive(s). The additives have included surfactants and inorganic or transition metal compounds (Joseph et al., 2013). Of the transition metal compounds, commercially available ferrocene ($FeCp_2$) shown in Fig. 1a is expected to become a new flame inhibitor, based on recent studies (Koshiba et al., 2015a). Linteris et al. (2000) first reported that 200-ppm ferrocene vapor significantly reduces the burning velocity of premixed methane/air flames. Furthermore, Koshiba et al. (2012) clearly demonstrated that even a low ferrocene fraction can extinguish a filter paper fire. However, these earlier studies also highlighted the issue of fire-suppression efficiency, which was found to decrease dramatically at high ferrocene fractions.

One approach to solve this issue is to employ an aqueous dispersion of ferrocene powder as a

suppressant. The benefit of this method lies in the ease of preparation of dispersions with optimum ferrocene concentrations using surfactants. In addition, aqueous dispersions offer the combined benefit of the suppression efficiencies of both water and ferrocene. In our previous study, the aqueous dispersions of ferrocene powder were prepared with a gemini surfactant (Koshiba, 2015b), which demonstrated that ferrocene dispersions have high suppression abilities; however, only one gemini surfactant was examined.

The main objectives of the present study were to experimentally elucidate the fire extinguishing ability of ferrocene dispersions containing gemini surfactants and to explore the relationship between the dispersibility and extinguishing capability for three gemini surfactants from the same series: olfin E1020, olfin PD 201, and surfynol 465 (see Fig. 1b). Their dispersibilities were characterized by both visual observations and turbidity measurements, whereas their fire suppression abilities were evaluated based on their fire extinguishing times for n-heptane pool fires. Aqueous ferrocene dispersions are also advantageous as they are phosphorus free and pose low environmental risks. The former characteristic is beneficial owing to the increasing cost and depletion risk of phosphate rock (Cordell and Neset, 2014), whereas the latter is a result of the halogen-free natures and low toxicities of these dispersions; ferrocene itself poses almost no environmental risk, as its toxicity is low and the primary products of the inhibition reaction are likely to be iron oxides. Surfynol 465 complies with Food and Drug Administration and Environmental Protection Agency regulations.

2. Material and Methods

2.1 Chemicals

Ferrocene was of reagent grade (>98.0%, Wako Pure Chem. Ind. Ltd., Japan). n-Heptane (> 99.9%, Kanto Chem. Co. Inc., Japan) was passed through molecular sieves to remove residual water. Deionized water (<1 μS/cm) was used. The three surfactants (i.e., olfin E1020, olfin PD 201, and surfynol 465) were purchased from Nissin Chem. Ind. Co. Ltd., Japan and were used as received.

As described above, olfin E1020, olfin PD201, and surfynol 465 are gemini surfactants, which can be viewed as bis-surfactants, where two amphiphilic molecules are connected by a short spacer (Holmberg, 2003). In general, gemini surfactants are highly efficient in lowering the critical micelle concentration (CMC) (Páhi et al., 2009). Olfin E1020 ($m + n = 20$) and surfynol 465 ($m + n = 30$) are 2,4,7,9-tetramethyl-5-decyne-4 and 7-diol-di(polyoxyethylene) ether, respectively, while olfin PD201 is a mixture consisting primarily of the ether and propylene glycol.

2.2 Preparation

2.2.1 Ferrocene milling procedures

Three ferrocene samples (S1–S3) were prepared to investigate the effects of ferrocene particle size on dispersibility and extinguishing time. Micron-sized ferrocene particles (yellow powder) were

prepared by wet-milling as-received ferrocene particles (light orange powder) in a planetary mill (Pulverisette 7, Fritsch, Germany) with ϕ 2 mm ZrO_2 balls. The particle size distributions of the ferrocene samples were determined by laser diffraction spectroscopy (SALD 7000, Shimadzu, Japan). The median diameters (d_{50}) of S1, S2, and S3 were determined to be 10.4, 11.4, and 21.5 μm, respectively.

2.2.2 Preparation of aqueous ferrocene dispersion

Milled ferrocene powder was added to an aqueous solution of the surfactant, whose surfactant concentration was set to twice the CMC value determined by the du Noüy ring method (du Noüy, 1925). Aqueous dispersions of ferrocene particles were prepared by ultrasonicating (43 kHz) for 20 min at 323 K. A temperature of 323 K is below the cloud point of the surfactants, which is the temperature at which phase separation occurs (ASTM D2024, 2013).

2.3 Characterization

2.3.1 Dispersibility

Visual observations and nephelometric measurements were conducted to gain insight into the dispersibilities of the aqueous ferrocene dispersions. Dispersibility is typically characterized as a function of the turbidity of the dispersion (Itami and Fujitani, 2005), where higher turbidity indicates

1 better dispersibility. The ferrocene concentration was set to 100 ppm on a mass/mass basis in these
2 experiments, which was the same as that used in our previous study (Koshiba et al., 2015b). In the
3 present study, the turbidity measurements (NTU for formazine) were conducted by a turbidimeter
4 (2100Q, Hach Co., USA) at room temperature. Prior to performing the turbidity measurements, the
5 turbidimeter was calibrated using 20, 100, and 800 NTU StablCal standards (Hach Co., USA). To
6 negate the ferrocene color, the turbidity was determined from the ratio of the 90° scattered light
7 signals to transmitted light signals.
8
9 *2.3.2 Suppression experiments*
10 The experimental setup for the suppression experiments, depicted in Fig. 2a, was the same as that
11 used for a preceding study (Koshiba et al., 2015b). The experimental apparatus was built to simply
12 investigate the effect of dispersibility on suppression capability. An 83-mm-diameter pan was used
13 with a nozzle placed 600 mm above it, which was connected to an electric high-pressure pump. For
14 each trial, 80 mL of n-heptane was poured into the pan and a free burn was conducted until a
15 quasi-steady burning rate was achieved. After preburning, the nozzle was activated at a flow rate of
16 250 mL/min. The average extinguishing times ($\bar{\tau}$) were determined in 10 fire-suppression trials per
17 ferrocene sample.
18 Prior to the suppression experiments, the full cone spray pattern properties were assessed. The

spray is typically characterized by water-flux distribution and droplet properties, namely, the droplet size, viscosity, specific gravity, temperature, and pressure (Santangelo et al., 2014). The temperature and pressure were kept constant in the present study. The viscosity and specific gravity were expected to have mminimal impacts on the droplet properties owing to the very low content of ferrocene (100 ppm) and surfactant (0.2–0.4 wt%) in the aqueous ferrocene dispersions. The droplets from the nozzle were directly collected in 73 jars (23 mm in diameter × 55 mm in height) to determine the volume flux distribution. The vessels were arranged in a radial pattern on the floor under the nozzle (see Fig. 2b). The average volume flux ($L/m^2 \cdot min$) decreased gradually with distance from the center (D, see Fig. 2c). The immersion method (Hurlburt and Hanratty, 2002) using silicone oil provided values for the Sauter mean diameter d_{32}, d_{v50}, and d_{v99} of 313, 207, 480 μm, respectively. Here, d_{32} was calculated using Eq. (1).

$$d_{32} = \sum(N_i d_i^3) / \sum(N_i d_i^2), \qquad (1)$$

where N_i is the measured number of droplets with diameter d_i. It should be noted that the droplet size can change as a result of the measurement method (Hurlburt and Hanratty, 2002); nevertheless, the size of the droplets produced in this study was substantially larger than that of ferrocene powder.

3. Results

3.1 Dispersibility

The aqueous ferrocene dispersions containing the gemini surfactants are shown in Fig. 3. The ferrocene–surfynol 465, ferrocene–olfin E1020, and ferrocene–olfin PD201 dispersions were poured into the left, center, and right test tubes, respectively, and the upper, middle, and lower digital pictures depict the dispersions of S1, S2, and S3 ferrocenes, respectively. Initially (i.e., at zero min, see left column), the dispersibility was negatively correlated with the ferrocene particle size, indicating that dispersibility improved as ferrocene particle size decreased. Even at zero min, a yellow ferrocene precipitate was observed at the bottom of the test tube when using the S3 ferrocene powder. At 240 min, the dispersibility was still found to be negatively correlated to the ferrocene particle size. Comparison of the dispersibilities among the surfactants revealed surfactant dependency, with the dispersibilities of the surfactants being ranked in the following order: surfynol 465 ≥ olfin E1020 > olfin PD201.

The turbidity of each sample was then measured to quantitatively evaluate its visually observed dispersibility. Fig. 4 shows the turbidity variations of the ferrocene dispersions versus time, and Table 1 summarizes the initial turbidities of the ferrocene dispersions. The nephelometric measurements clearly demonstrated that the initial turbidity order completely coincided with the dispersibility order obtained from the visual observations; specifically, increasing the ferrocene

particle size decreased the turbidity (i.e., dispersibility). In addition, the surfactant likely dominated the dispersibilities of the aqueous ferrocene dispersions, with the following dispersibility order: surfynol 465 ≥ olfin E1020 > olfin PD201. This result is in good agreement with the visual observations.

3.2 Suppression experiments

Before performing the suppression experiments with the ferrocene dispersions, we confirmed that the pure water mist and aqueous solutions of the surfactant (at twice the concentration of the CMC) were unable to suppress pool fires. Fig. 5 shows the extinguishing times of the aqueous dispersions of ferrocene particles. For reference, the extinguishing time of a 45 wt% aqueous solution of potassium carbonate (a conventional wet chemical agent) is also shown. As seen in the figure, the ferrocene dispersions offered significantly shorter extinguishing times and smaller standard deviations than the conventional extinguishing agent (τ = 12.9 s, *SD* = 5.9 s). For the dispersions tested, with the exception of the ferrocene–olfin E1020 dispersions, the extinguishing times appeared to be diameter independent: τ = 4.4 s, τ = 3.7 s, τ = 5.1 s for the S1, S2, and S3 ferrocene–olfin PD201 dispersions, respectively. For the same ferrocene samples, the extinguishing times exhibited the following order: ferrocene dispersion containing PD201 > ferrocene dispersion containing olfin E1020 ≥ ferrocene dispersion containing surfynol 465. In other words, the surfactants can be ranked

in the following order in terms of their fire-extinguishing capabilities: ferrocene dispersion containing surfynol 465 ≥ ferrocene dispersion containing olfin E1020 > ferrocene dispersion containing PD201.

4. Discussion

Aqueous ferrocene dispersions are expected to be effective fire-extinguishing agents. As such, the main focus of the present study was to investigate the relationship between their dispersibilities and extinguishing efficiencies. To accomplish this objective, we investigated the dispersibilities and extinguishing times of ferrocene dispersions containing gemini surfactants from the same series, namely, olfin E1020, olfin PD201, and surfynol 465. All the tested aqueous dispersions, which contained only 100-ppm ferrocene, had significantly shorter extinguishing times than the conventional wet chemical agent containing at least 45-wt% potassium carbonate. Regrettably, only one conventional extinguishing agent was tested in the present work. We detected an interesting trend in the visual observations and turbidity measurements, in that the dispersibility order was strongly surfactant-dependent, with surfynol 465 ≥ olfin E1020 > olfin PD201.

4.1 Relationship between extinguishing efficiency and dispersibility

Fig. 6 illustrates the extinguishing times versus the initial turbidities of the ferrocene dispersions.

The initial turbidities were considered since the dispersion was discharged immediately after preparation. The resulting plots are approximately linear, with a Pearson correlation coefficient of −0.95 and a high coefficient of determination of 0.90, indicating that the extinguishing time consistently increases with initial turbidity. It should be noted that the extinguishing time likely varies linearly with respect to the initial turbidity within these ranges. As described above, no pool fires were extinguished (i.e., $\tau = \infty$) when dispersions with initial turbidities of zero (i.e., aqueous solution of the surfactant) were used. Hence, the linear relationship between the extinguishing time and the initial turbidity does not hold when the initial turbidity is approximately zero.

As depicted in Fig. 6, the extinguishing time linearly decreases with increasing initial turbidity. In particular, as shown in Figs. 4 and 5, the dispersions containing olfin PD201, which exhibited poor dispersibility, have long extinguishing times and large standard deviations. These characteristics are most likely evident because the surfactant governs the dispersibility, which is positively correlated with the fire extinguishing efficiency.

In a flame, it is known that the suppression efficiency of iron compounds is strongly influenced by the inhibiting iron species, such as Fe, FeO, FeO_2, FeOH, and $Fe(OH)_2$ (Linteris et al., 2008). The radical recombination pathways shown in Fig. 7 were suggested for iron pentacarbonyl; however, ferrocene likely has the same recombination mechanism as iron pentacarbonyl, as the these iron complexes readily decompose at relatively low temperatures to yield iron species (Fondell et al.,

2015, Andrews et al., 1999, Tepe et al., 1998). The inhibiting species, in excess of their super-equilibrium concentrations, are highly effective at scavenging radicals; however, experimental and numerical studies have demonstrated that a very high iron species fraction in a flame causes the condensation and agglomeration of the iron species, resulting in a decrease in the fire extinguishing capability. Needless to say, a low iron species fraction cannot suppress a flame. Poor dispersibility implies that the ferrocene particles are heterogeneously distributed in water, thus producing both locally concentrated and dilute sites. As described above, inhibiting iron species are not effective at catalytically recombinating radicals, such as H and OH, even if the iron species concentration is extremely high or low. Hence, it is probable that dispersions with poor dispersibilities exhibit longer extinguishing times and larger standard deviations.

4.2 Effects of ferrocene particle size and surfactant on extinguishing efficiency

Two-way analyses of variance (two-way ANOVAs) were conducted to quantitatively examine the main effects of ferrocene particle size (S1–S3) and surfactant (surfynol 465, olfin E1020, and olfin PD201) and their two-way interaction (i.e., ferrocene particle size × surfactant). Before performing the two-way ANOVAs, all data were log-transformed to ensure homoscedasticity with Levene's test (Heredia-Guerrero et al., 2014). In the statistical analyses, differences were considered to be significant when $p < 0.05$. A two-way ANOVA revealed no significant ferrocene particle size ×

surfactant interaction. Hence, the main effects of ferrocene particle size and surfactant are hereafter addressed.

4.2.1 Main effect of ferrocene particle size on extinguishing time

A two-way ANOVA revealed no significant main effect of ferrocene particle size on extinguishing time ($F = 2.129$, $p = 0.1256$). Therefore, in the 10.4–21.5 μm ferrocene diameter range, the ferrocene particle size negligibly influenced the extinguishing times when used with the gemini surfactants tested in this study.

Typically, the particle size of a suppressant strongly governs its fire extinguishing ability (Ewing et al., 1995). Assuming that all fine ferrocene particles are spherical, the surface area of each S1 particle (with d_{50} = 10.4 μm) was 4.2 times greater than that of each S3 particle (with d_{50} = 21.5 μm). However, no significant effect of ferrocene particle size on extinguishing time was detected, which may be due to the ease of the ferrocene decomposition in the gas phase. In fact, the pseudo-first-order decomposition of ferrocene occurs at relatively low temperatures (> 673 K) when the ferrocene fraction is orders of magnitude lower than the oxygen fraction (Lubej and Plazl, 2014). This suggests that the mean ferrocene particle size in the dispersion system needs not be less than 20 μm when the long-term stability of the dispersion is not a concern.

4.2.2 Main effect of surfactant on extinguishing time

A two-way ANOVA revealed a significant main effect of the surfactant on the extinguishing time ($F = 49.516$, $p < 0.001$). *Post hoc* Tukey's HSD (honest-significant difference) multiple comparison (Souza-Alonso et al., 2015) revealed significant differences between the extinguishing times of the surfactants (all $p < 0.001$), and the extinguishing capability order was as follows: dispersions containing surfynol 465 > dispersions containing olfin E1020 > dispersions containing olfin PD201. This implies that the dispersibility significantly depends on the surfactant used. As a result, the suppression abilities of ferrocene dispersions exhibited surfactant dependences.

4.3 Other advantages over conventional fire extinguishing agents

The price per gram of ferrocene is approximately three times higher than that of potassium carbonate; however, the amount of ferrocene required to extinguish a flame is approximately three orders of magnitude lower than that of potassium carbonate, suggesting that the total cost may be lower when employing ferrocene as an extinguishing agent.

Note that the extinguishing times of aqueous ferrocene dispersions may vary depending on the experimental conditions (e.g., ferrocene concentration, droplet size, and fire source) (Ewing et al., 1995), and the chemical stability of ferrocene in water was not investigated in this study. However, the present study suggests that halogen- and phosphorous-free, less-toxic fire-extinguishing agents

exhibit fire extinguishing performances superior to those of conventional extinguishing agents for Class-B fires. In addition, we found that the ferrocene powder dispersibility significantly influences fire extinguishing efficiency.

5. Concluding Remarks

To evaluate the fire extinguishing performances of aqueous ferrocene dispersions and to explore the relationship between their dispersibilities and extinguishing efficiencies, visual observations, nephelometric measurements, and fire-suppression experiments were conducted using gemini surfactants from the same series, namely, olfin E1020, olfin PD201, and surfynol 465. The main results obtained from this work are as follows:

(1) The extinguishing times of aqueous ferrocene dispersions were shorter than those of a 45-wt% aqueous solution of potassium carbonate (a conventional wet chemical agent).

(2) In the ferrocene diameter range of 10.4–21.5 μm, a two-way ANOVA clearly indicated that the ferrocene diameter negligibly influenced the extinguishing time when used with the gemini surfactants.

(3) For the same ferrocene sample, the extinguishing ability order was as follows: ferrocene dispersion containing surfynol 465 > ferrocene dispersion containing olfin E1020 > ferrocene

dispersion containing olfin PD201.

(4) The extinguishing times of the ferrocene dispersions were negatively correlated with their initial turbidities, indicating that there was a positive and linear relationship between their extinguishing capabilities and the dispersibilities. This discovery is of great importance for enhancing the fire-suppression performances of ferrocene dispersions.

In conclusion, we were able to elucidate the effects of dispersibility on the fire extinguishing capabilities of aqueous ferrocene dispersions. These dispersions' abilities to suppress Class B fires and their halogen- and phosphorus-free natures confirm that ferrocene is effective as a new water mist additive.

Acknowledgments

This work was supported by the Japan Society for the Promotion of Science (JSPS) KAKENHI, Grant No. 25750135 to Y.K. We thank Mr. K. Iida, who contributed to the suppression experiments. We are also grateful to the Instrumental Analysis Center, Yokohama National University for conducting the microscopic observations in the immersion measurements.

References

Andrews, R., Jacques, D., Rao, A.M., Derbyshire, F., Qian, D., Fan, X., Dickey, E.C., Chen, J., 1999. Continuous production of aligned carbon nanotubes: a step closer to commercial realization. Chem. Phys. Lett. 303, 467–474.

ASTM D2024−09, 2013. Standard test method for cloud point of nonionic surfactants, Vol. 15. 04, West Conshohocken, PA.

Cordell, D., Neset, T.-S.S., 2014. Phosphorus vulnerability: a qualitative framework for assessing the vulnerability of national and regional food systems to the multidimensional stressors of phosphorus scarcity. Glob. Environ. Change 24, 108–122.

du Noüy, P.L., 1925. An interfacial tensiometer for universal use. J. Gen. Physiol. 7, 625–633.

Ewing, C.T., Faith, F.R., Romans, J.B., Siegmann, C.W., Ouellette, R.J., Hughes, J.T., Cathart, H.W., 1995. Extinguishing class B fires with dry chemicals: Scaling studies. Fire Technol. 31, 17–43.

Fire and Disaster Management Agency, 2014. Annual report on facilities with dangerous materials. Safety & Tomorrow 156, 33–37 (in Japanese).

Fondell, M., Johansson, F., Gorgoi, M., von Fieandt, L., Boman, M., Lindblad, A., 2015. Phase control of iron oxides grown in nano-scale structures on FTO and Si(100): Hematite, maghemite and magnetite. Vacuum 117, 85–90.

Heredia-Guerrero, N., Oliet J.A., Villar-Salvador P., Benito, L.F., Peñuelas J.L., 2014. Fertilization regime interacts with fall temperature in the nursery to determine the frost and drought tolerance of the Mediterranean oak Quercus ilex subsp. Ballota. For. Ecol. Manage. 331, 50–59.

Holmberg, K., Jönsson, B., Kronberg, B., Lindman, B., 2003. Surfactants and polymers in aqueous solution, second ed. John Wiley & Sons, Ltd, Chichester.

Hurlburt, E.T., Hanratty, T.J., 2002. Measurement of drop size in horizontal annular flow with the immersion method. Exp. Fluids 32, 692–699.

Itami, K., Fujitani, H., 2005. Change characteristics and related dispersion/flocculation behavior of soil colloids as the cause of turbidity. Colloid Surf. A Physicochem. Eng. Asp. 265, 55–63.

Jenft, A., Collin, A., Boulet, P., Pianet, G., Breton, A., Muller, A, 2014. Experimental and numerical study of pool fire suppression using water mist. Fire Saf. J. 67, 1–12.

Joseph, P., Nichols, E., Novozhilov, V., 2013. A comparative study of the effects of chemical additives on the suppression efficiency of water mist. Fire Saf. J. 58, 221–225.

Koshiba, Y., Agata, S., Takahashi, T., Ohtani, H., 2015a. Direct comparison of the flame inhibition efficiency of transition metals using metallocenes. Fire Saf. J. 73, 48–54.

Koshiba, Y., Iida, K., Ohtani, H., 2015b. Fire extinguishing properties of novel ferrocene/surfynol 465 dispersions. Fire Saf. J. 72, 1–6.

Koshiba, Y., Takahashi, Y., Ohtani, H., 2012. Flame suppression ability of metallocenes (nickelocene, cobaltocene, ferrocene, manganocene, and chromocene). Fire Saf. J. 51, 10–17.

Kuang, K., Huang, X., Liao, G, 2008. A comparison between superfine magnesium hydroxide powders and commercial dry powders on fire suppression effectiveness. Process Saf. Env. Prot. 86, 182–188.

Linteris, G.T., Rumminger, M.D., Babushok, V.I., 2008. Catalytic inhibition of laminar flames by transition metal compounds. Prog. Energy Combust. Sci. 34, 288–329.

Linteris, G.T., Rumminger, M.D., Babushok, V., Tsang, W., 2000. Flame inhibition by ferrocene and blends of inert and catalytic agents. Proc. Combust. Inst. 28, 2965–2972.

Lubej, M., Plazl, I., 2014. Theoretical and experimental study of iron catalyst preparation by chemical vapor deposition of ferrocene in air. Chem. Eng. J. 242, 306–312.

Páhi, A.B., Királya, Z., Puskás, S., 2009. Mass spectrometric characterization of the non-ionic gemini surfactant Surfynol 465 and a microcalorimetric study of its micelle formation in water. Colloid Surf. A Physicochem. Eng. Asp. 345, 13–17.

Santangelo, P.E., Jacobs, B.C., Ren N., Sheffel, J.A., Corn, M.L., Marshall, A.W., 2014. Suppression effectiveness of water-mist sprays on accelerated wood-crib fires. Fire Saf. J. 70, 98–111.

Souza-Alonso, P., Guisande-Collazo, A., González, L., 2015. Gradualism in Acacia dealbata Link

invasion: Impact on soil chemistry and microbial community over a chronological sequence. Soil Biol. Biochem. 80, 315–323.

Tepe, R.K., Jacksier, T., Barnes, R.M., 1998. Determination of iron and nickel in electronic grade chlorine by sealed inductively coupled plasma atomic emmision spectrometry. J. Anal. At. Spectrom. 13, 989–994.

Wang, P., 2014. Application of green surfactants developing environment friendly foam extinguishing agent. Fire Technol. 10.1007/s10694-014-0422-5.

Figure captions

Figure 1

Chemical structures of (a) ferrocene, (b) olfin E1020 ($m + n = 30$), and (c) surfynol 465 ($m + n = 20$).

Figure 2

(a) Experimental apparatus for the fire suppression tests. (b) Arrangement of 73 cylindrical vessels for volume flux measurements. (c) Average volume flux as function of distance from spray center (D).

Figure 3

Digital photographs of aqueous ferrocene dispersions. Left, center, and right test tubes contain surfynol 465, olfin E1020, and olfin PD201, respectively. Upper, middle, and lower photographs show aqueous dispersions of S1, S2, and S3 ferrocenes, respectively. For interpretation of the references to color in this figure legend, the reader is referred to the web version of this article.

Figure 4

Turbidities of the aqueous ferrocene dispersions versus time (circles = dispersions containing surfynol 465, triangles = dispersions containing olfin E1020, and squares = dispersions containing olfin PD201). (a) S1 ferrocene, (b) S2 ferrocene, and (c) S3 ferrocene.

Figure 5

Extinguishing times of the aqueous ferrocene dispersions (circles = dispersions containing surfynol 465, triangles = dispersions containing olfin E1020, and squares = dispersions containing olfin PD201) and 45-wt% aqueous potassium carbonate solution (lozenge). Error bars indicate standard deviations. a: adapted from Koshiba et al. (2015b).

Figure 6

Extinguishing time versus initial turbidity. Fitting performing by linear least-squares method.

Figure 7

Schematic diagram of radical recombination mechanism for iron species (adapted from Linteris et al. (2008)).

Table caption

Table 1

Initial turbidity values of ferrocene dispersions.

Table 1

Ferrocene	Initial turbidity (NTU)		
	Ferrocene dispersion containing olfin E1020	Ferrocene dispersion containing olfin PD201	Ferrocene dispersion containing surfynol 465
S1	167.1	159.8	125.8
S2	133.1	130.8	104.8
S3	45.7	48.4	25.2

Figure 1a

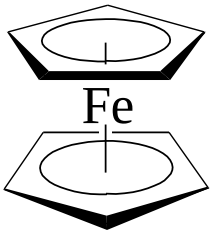

Figure 1b

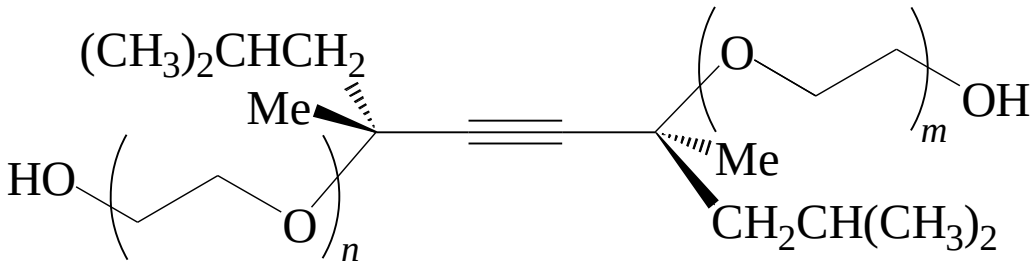

Figure 2a

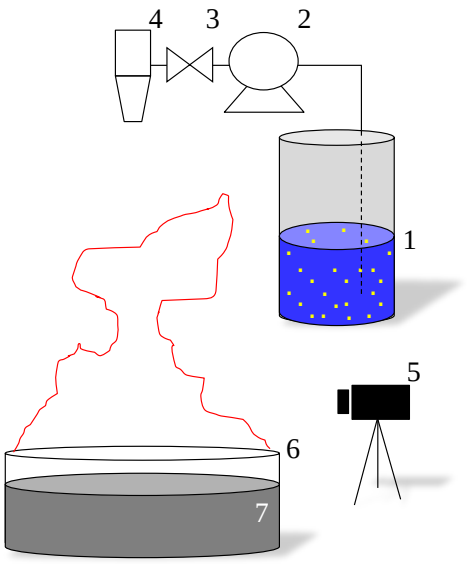

1. suppressant, 2. pump, 3. valve,
4. nozzle, 5. camera, 6. pan, 7. n-heptane.

Figure 2b

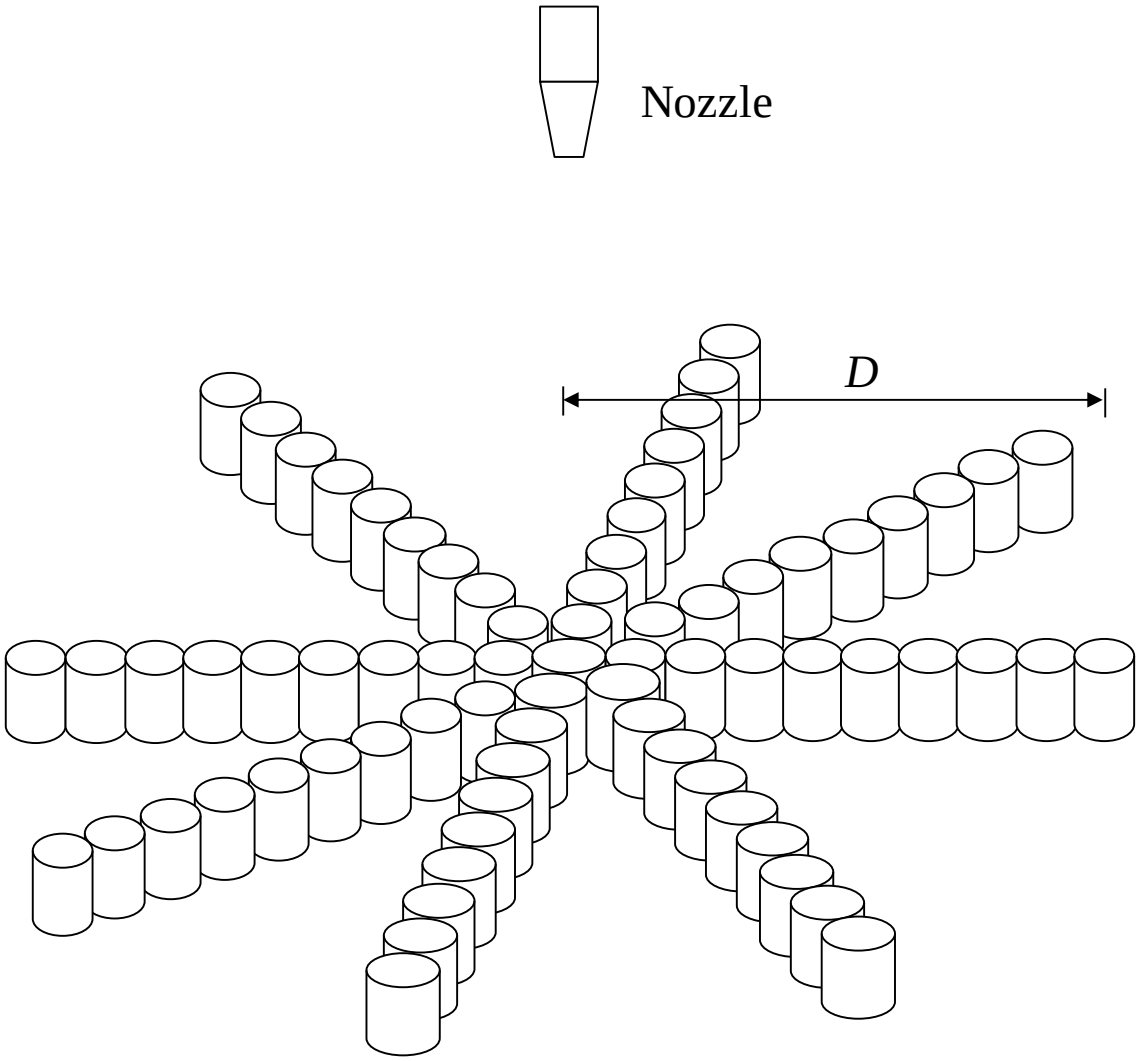

Figure 2c

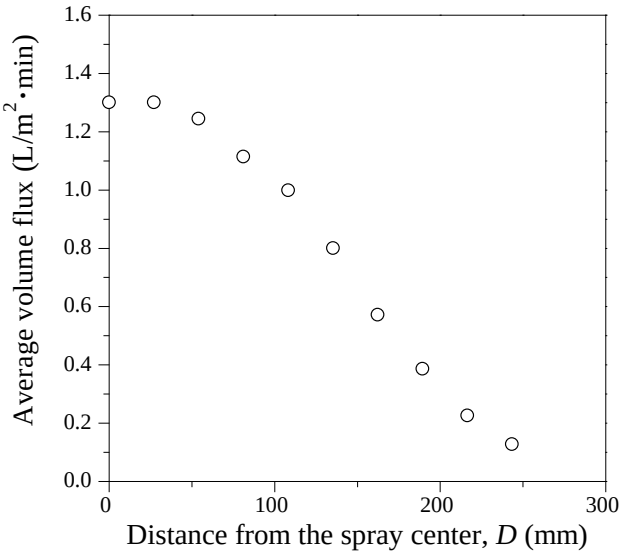
Average volume flux (L/m^2·min)
1.6
1.4
1.2
1.0
0.8
0.6
0.4
0.2
0.0
0
100
200
300
Distance from the spray center, *D* (mm)

Figure 3

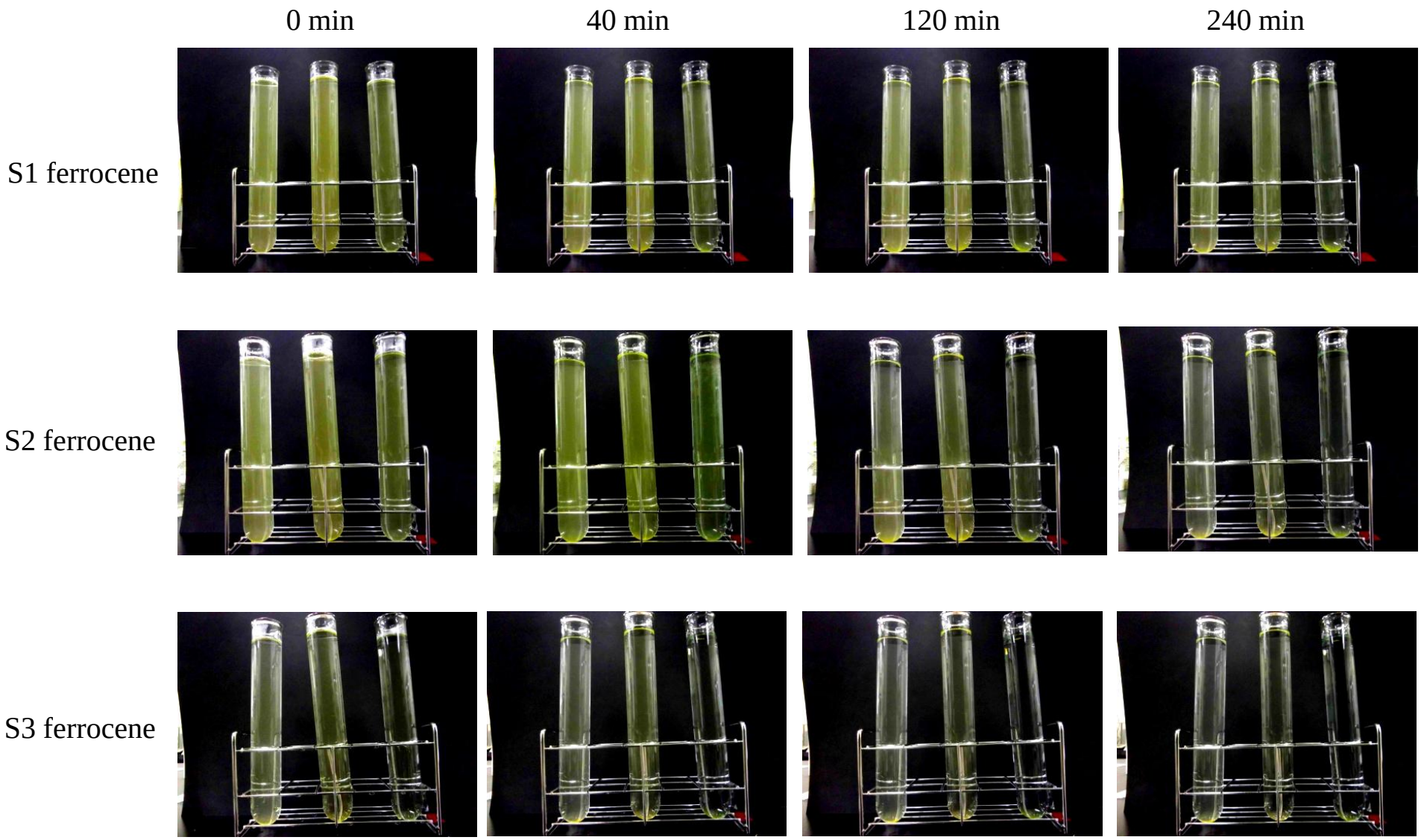
0 min
40 min
120 min
240 min
S1 ferrocene
S2 ferrocene
S3 ferrocene

Figure 4a

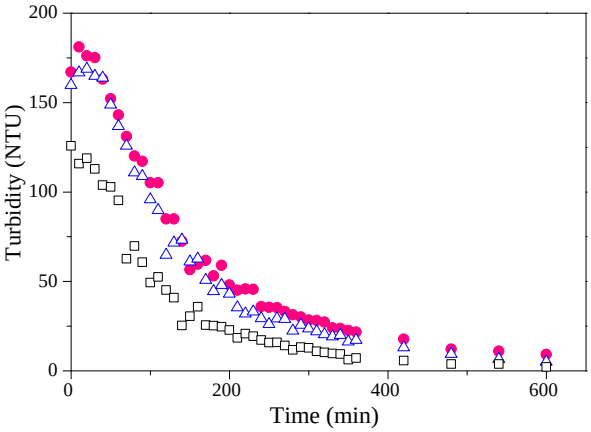

Figure 4b

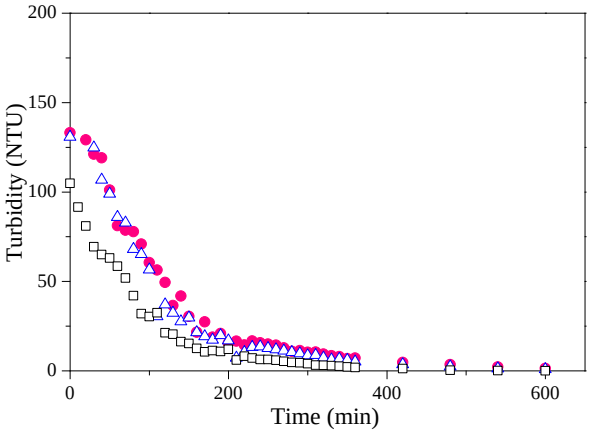

Figure 4c

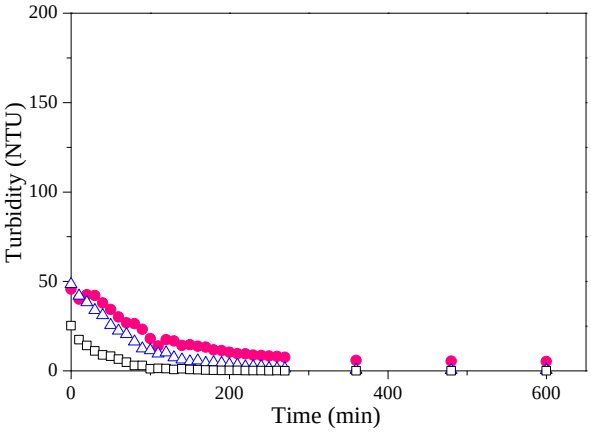

Figure 5

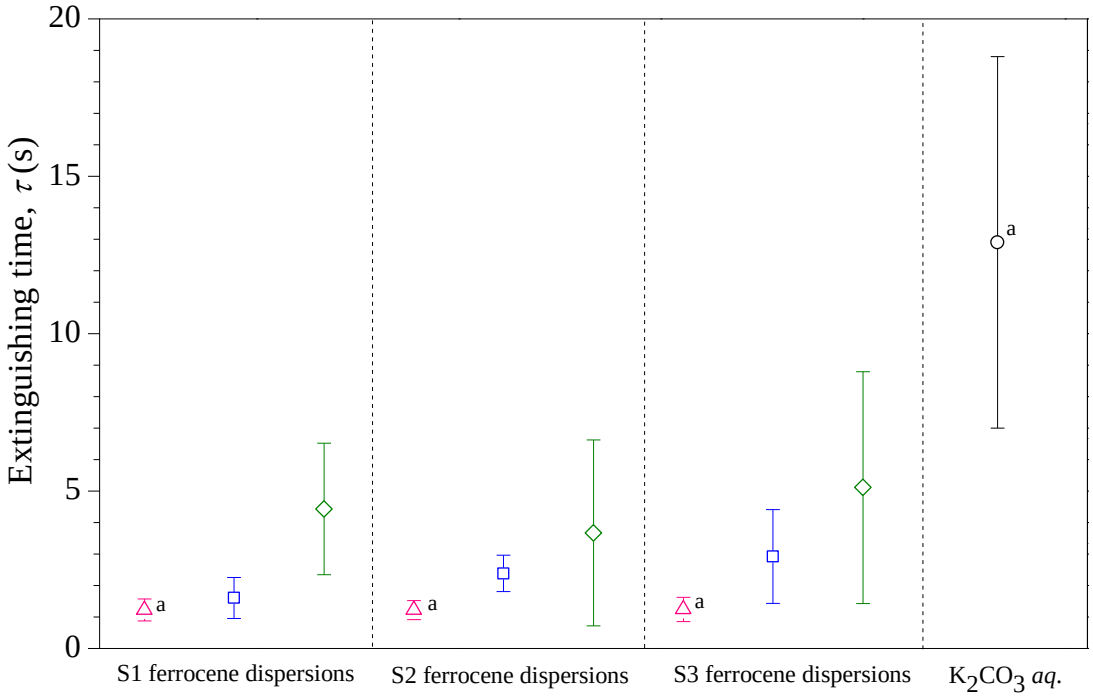
20
15
10
5
0
Extinguishing time, τ (s)
a
a
a
a
S1 ferrocene dispersions
S2 ferrocene dispersions
S3 ferrocene dispersions
K2CO3 aq.

Figure 6

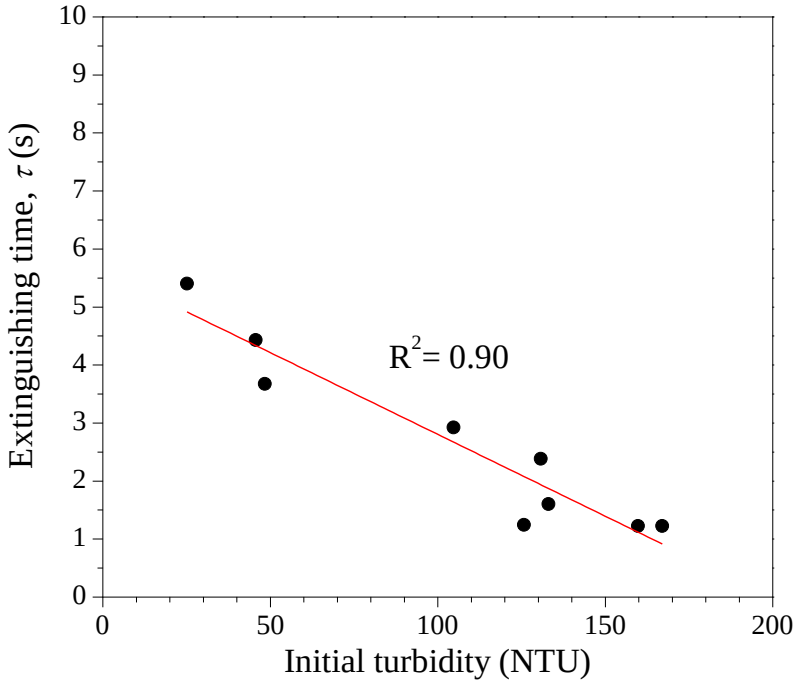
Extinguishing time, τ (s)
Initial turbidity (NTU)
R²= 0.90
0
1
2
3
4
5
6
7
8
9
10
0
50
100
150
200

Figure 7